Mon. Not. R. Astron. Soc. **268,** 159–168 (1994)

Amplified electrostatic transverse waves in pulsar magnetospheres

Qinghuan Luo,[1] D. B. Melrose[1] and G. Z. Machabeli[2]

[1] *Research Centre for Theoretical Astrophysics, School of Physics, University of Sydney, NSW 2006, Australia*
[2] *Abastumani Astrophysical Observatory, Kazbegi Ave 2a, Tbilisi, Georgia*

Accepted 1993 December 6. Received 1993 December 3; in original form 1993 July 27

ABSTRACT

The natural modes of a relativistic, dense pair plasma streaming along field lines consist of electrostatic transverse waves (the subluminal branch of the ordinary mode) and purely transverse waves (the extraordinary mode). In the case of a strong, uniform magnetic field, the beam–plasma instability can occur only for longitudinal waves propagating along the field lines. It is shown that, when curvature drift is included, a beam–plasma instability of the 'hydrodynamic' type can occur for electrostatic transverse waves. Possible applications to pulsar radio emission are discussed. It is shown that the instability for longitudinal waves propagating along the field lines can be suppressed by curvature drift when the Lorentz factor of the beam particles is large. This upper limit on the Lorentz factor for instability to occur is derived.

Key words: instabilities – plasmas – radiation mechanisms: non-thermal – pulsars: general.

1 INTRODUCTION

Despite several decades of investigations, there is no consensus on the specific radiation mechanism that is involved in pulsar radio emission. It is widely accepted that the emission must involve some form of instability, but there are numerous possible instabilities, and opinions vary as to which is the most favourable. In this paper we consider only instabilities that occur well within the pulsar magnetosphere, specifically excluding processes near and outside the light cylinder. With this restriction, the cyclotron frequencies of electrons and positrons are well above the radio range, and processes involving cyclotron resonances are not relevant. Even with this restriction there are three broad classes of instabilities and a large number of specific instabilities that have been discussed in the literature. The broad classes include (i) the old idea of a bunching instability and an antenna emission process (Sturrock 1971; Sturrock, Petrosian & Turk 1975; Ruderman & Sutherland 1975), (ii) maser emission processes (Zheleznyakov & Shaposhnikov 1979; Chugunov & Shaposhnikov 1988; Luo & Melrose 1992b, hereafter LM; Luo 1993a), in which the dispersion properties of the ambient plasma are unimportant (the refractive index n is approximated by unity), and (iii) instabilities in a dense pair plasma, in which the dispersive properties of the ambient plasma play a central role (with $n \neq 1$). Every instability requires a source of free energy, for which there is a variety of possibilities, including (a) streaming of a very energetic (primary) beam through a pair plasma (Ruderman & Sutherland 1975); (b) relative streaming of electrons and positrons (Cheng & Ruderman 1977); (c) inhomogeneities in the plasma, including both faster particles from a following bunch overtaking slower particles from a preceding bunch (Usov 1987) and boundary effects (Asseo, Pellat & Sol 1983, hereafter APS; Larroche & Pellat 1987); (d) inhomogeneities in the magnetic field, due to curvature and torsion of field lines (Blandford 1975; Luo 1993a), and (e) drift of particles across the field lines (LM, and references therein).

In this paper we are concerned with instabilities that involve curvature of the fields and associated drift across the field lines ('curvature drift'). In principle these effects can lead to instabilities both of the maser type, with $n=1$, and of the 'hydrodynamic' type, in which plasma dispersion is essential. It was pointed out by Zheleznyakov & Shaposhnikov (1979) that a maser-type instability is possible when curvature drift is taken into account (cf. also Chugunov & Shaposhnikov 1988; Luo & Melrose 1992a; LM). No maser action is possible when curvature drift is neglected (Blandford 1975; Melrose 1978; Machabeli 1991). It follows that no maser action is possible in the formal limit of an infinite magnetic field ($B \rightarrow \infty$), due to the drift velocity ($v_{\rm d} \propto 1/B$) vanishing in this limit. A hydrodynamic instability can develop as a result of curvature drift, as discussed in detail below. One expects the hydrodynamic and maser instabilities to be related, in the sense that they are opposite limiting cases of a single more general instability (Melrose 1986), and on the basis of this one would expect the hydrodynamic instability to vanish in the limit $B \rightarrow \infty$. In contrast, Beskin, Gurevich & Istomin (1988, hereafter BGI) claimed that such an instability can occur in the limit $B \to \infty$, and their claim has led to controversy (Nambu 1989; Machabeli 1991; BGI).

The paper is organized as follows. In Section 2, some properties of the pair plasma of a pulsar magnetosphere are summarized. In Section 3, we show that an instability of 'hydrodynamic' type, driven by curvature drift, can occur for electrostatic transverse waves (the subluminal branch of the ordinary mode) in a dense pair plasma with an energetic beam. The limiting case $B \to \infty$ is also discussed. It is shown that, in the infinite magnetic field limit, as in the case discussed by BGI, an instability cannot develop. In Section 4, it is shown that the usual hydrodynamic instability (as in uniformly magnetized plasma) for Langmuir waves propagating along field lines can be suppressed by the curvature drift effect if the Lorentz factor of the particle beam is large. In Section 5, the instability theory developed in Section 3 is applied to radio pulsars. Conclusions and a discussion are presented in Section 6.

2 WAVE MODES IN A PULSAR MAGNETOSPHERIC PLASMA

2.1 Magnetospheric plasma

Magnetospheric models that feature a dense outflowing pair plasma (e.g. Arons 1981) appear plausible. Such a pair plasma, which is penetrated by the primary beam, is relativistic and strongly magnetized. In the following discussion the pair plasma is also called the background plasma (as opposed to the beam). To describe such a beam–plasma (the background and primary beam) system, one may use either the laboratory frame that is associated with the star or the comoving frame in which the background plasma is at rest. In the laboratory frame the background plasma has a typical Lorentz factor of about $\gamma_p = 10^2$–10^3, while the Lorentz factor of the beam particles can be as high as $\gamma_b = 10^7$ (e.g. Ruderman & Sutherland 1975; Arons 1981). Specific values of both γ_p and γ_b are model-dependent. Nevertheless, in the cold plasma approximation, one can assume the following equipartition condition: $N_p\gamma_p \approx N_b\gamma_b$ in the laboratory frame, where N_p and N_b are the particle densities of the background (pair) and beam plasmas, respectively.

In reality, due to the broad distribution of parallel momenta, the energy of the pair plasma also has a broad distribution. For convenience, one usually introduces a dimensionless momentum $p_\varphi = \gamma v_\varphi / c$, where γ is the Lorentz factor and v_φ is the parallel (to the magnetic field line) velocity. When curvature drift is ignored, p_φ can be related to the Lorentz factor by $\gamma^2 \approx 1 + p_\varphi^2$. Let $f(p_\varphi)$ be the distribution of parallel momenta for the pair plasma. As pointed out by Arons (1981), $f(p_\varphi)$ features a power law with index $\lesssim -1.5$, followed by a plateau extending up to $p_\varphi^{max} = 10^3$–10^4. The lower cut-off of the distribution is $p_\varphi^{min} = 10$–50. Outside the interval $[p_\varphi^{min}, p_\varphi^{max}]$ the distribution drops off exponentially. Normally, due to the presence of the primary beam and the neutrality of the whole beam–plasma system, the distributions of electrons and positrons are not the same and are shifted relative to each other (Cheng & Ruderman 1977). For a beam–plasma instability (due to such a relative motion) to occur the parallel momentum spread is required to be much smaller than the mean difference between the momenta of each species. Because of the large momentum dispersion (e.g. Arons 1981), this condition may not be satisfied and the instability due to the relative motion can be suppressed. In the following discussion, we assume that such a distribution difference is negligible.

2.2 Wave modes

In plasma theory, the wave modes (the waves that can be supported in the plasma) are determined in terms of the response tensor. In the linear theory, the response tensor describes the response of a plasma to a perturbation field. In general, the response tensor for such a plasma is exceedingly cumbersome (Melrose & Stoneham 1977; Kirk 1980; Melrose 1980), and in practice simplifications must be made. One simplification made here is to neglect cyclotron effects. Another simplification is to neglect the vacuum polarization contribution. Let $\varepsilon = 10^{-4}$–1 be the fraction of the cross-cap potential drop contained in the total potential drop developed along the magnetic field line near the surface of the star (the lowest value corresponds to the Crab pulsar). The criterion for neglecting the vacuum polarization effect can then be conveniently written (Arons & Barnard 1986) $\varepsilon(r/R_L)^3 \gg (\alpha_f/45\pi)(B/B_c)^2$, where r is the distance to the star, R_L is the light cylinder distance, $\alpha_f = e^2/4\pi\varepsilon_0\hbar c \approx 1/137$ is the fine-structure constant and $B_c = m_e^2c^2/e\hbar \approx 4.4 \times 10^9$ T is the critical magnetic field. This criterion is assumed to be satisfied.

To describe the wave properties of the pair plasma, the field lines are assumed to be locally circular, and hence it is convenient to use cylindrical coordinates (φ, r, z), in which the coordinate axis $\boldsymbol{e}_\varphi$ is along the field line, $\boldsymbol{e}_z$ is normal to the plane of the field line and $\boldsymbol{e}_r = \boldsymbol{e}_\varphi \times \boldsymbol{e}_z$. The three components of the wave vector $\boldsymbol{k}$ are represented by k_φ, k_r and k_z, respectively. The wave properties are determined by wave equations that include the current of the linear response to the perturbed field. In the case of a weak inhomogeneity, the perturbed field is given by $\boldsymbol{E}(\boldsymbol{x}, t) = \mathscr{E}(\boldsymbol{x}, t)\exp[-\mathrm{i}(\omega t - \boldsymbol{k}\cdot\boldsymbol{x})]$, where $\mathscr{E}(\boldsymbol{x}, t)$ depends weakly on $\boldsymbol{x}$ and t (cf. Appendix A). Let λ be the characteristic wavelength and R_B be the radius of curvature of the field lines. In the pulsar magnetosphere, one can assume that λ/R_B is small. On neglecting the terms of order λ/R_B, and assuming $|k_r/k| \ll |k_z/k|$, the dispersion equations are given by

$$1 - n^2 = 0 \tag{1}$$

and

$$(K_{zz} - n_{\varphi\varphi}^2)(K_{\varphi\varphi} - n_{zz}^2) - (n_{z\varphi}^2 - K_{z\varphi})^2 = 0 \tag{2}$$

(Lominadze et al. 1986; Asseo, Pellat & Sol 1990), with $n^2 = k^2c^2/\omega^2$ $(k = \boldsymbol{k}/|\boldsymbol{k}|)$, $n_{\varphi\varphi}^2 = k_\varphi^2c^2/\omega^2$, $n_{z\varphi}^2 = k_zk_\varphi c^2/\omega^2$ and $n_{zz}^2 = k_z^2c^2/\omega^2$. The response tensor components are represented by $K_{\varphi\varphi}$, $K_{z\varphi}$ and K_{zz}, respectively. The full expression for the response tensor including curvature drift can be derived by the method first proposed by Kazbegi et al. (1989), i.e. it is assumed that $\omega/\omega_B\gamma \ll 1$, where $\omega_B = eB/m_e$ is the non-relativistic gyrofrequency, and the perturbation is introduced along the field line. The only transverse perturbed motion is along $\pm\boldsymbol{e}_z$ via the drift angle θ_d, which is in turn determined by the parallel motion. Thus $K_{z\varphi}$ and K_{zz} are smaller than $K_{\varphi\varphi}$ by at least a factor of θ_d. In a magnetospheric model that consists of a background pair plasma and a beam, the beam is usually assumed to be less dense than the background plasma (but more energetic), so that the wave dispersion is dominated by the response tensor of the background. Curvature drift is important only when the Lorentz factor satisfies the condition

$$\gamma^2 \Delta\theta\theta_d > 1 \tag{3}$$

(LM), where $\Delta\theta$ is the angular range of $\boldsymbol{k}$ with respect to the field line. In the case relevant to pulsar radio emission, one assumes $\Delta\theta < 1$. In (3), $\theta_d = v_d/v_\varphi$ is the drift angle, where $v_d = v_\varphi^2 \gamma/\omega_B R_B$ is the drift velocity (Luo & Melrose 1992a). For the pair plasma (as opposed to the beam) in a pulsar magnetosphere, condition (3) is not satisfied and curvature drift can be neglected in determining the wave properties. Thus, in determining the wave modes, one can use the approximation $K_{zz} \approx K_{z\varphi} \approx 0$, and $K_{\varphi\varphi}$ is given by

$$K_{\varphi\varphi} = 1 + \frac{\omega_p^2}{\omega^2} \int dp_\varphi \frac{\beta_\varphi \omega}{\omega - k_\varphi v_\varphi} \frac{\partial f(p_\varphi)}{\partial p_\varphi}, \tag{4}$$

where ω_p is the non-relativistic plasma frequency of the pair plasma. We assume that the electrons and positrons have the same distribution $f(p_\varphi)$.

In analogy to the magnetoionic theory, the waves described by (1) and (2) may be identified as the extraordinary and ordinary modes, respectively. The extraordinary waves are transverse waves with an electric field vector in the $\boldsymbol{e}_r$ direction. These waves have a vacuum-like dispersion relation. This is expected because at any instant the particles move perpendicular to $\boldsymbol{e}_r$ and do not interact with the electric field of waves in that direction.

The ordinary-mode waves described by (2) can be classified as superluminal waves, whose phase speed exceeds c, and subluminal waves, with phase speeds less than c. For superluminal waves the Cerenkov resonance condition cannot be satisfied, and wave damping or growth by this resonance interaction mechanism is not possible. Thus any damping or growth of this type of wave must involve higher order interaction (e.g. scattering processes) between particles and waves. The case of single-particle motion in a superluminal wave was discussed by Rowe (1992). In the following discussion we only consider subluminal waves. Since these waves have an electric vector in the $\boldsymbol{e}_\varphi$–$\boldsymbol{e}_z$ plane and usually have an electric field component along $\boldsymbol{k}$, we will simply call them electrostatic transverse waves (they are also called Alfvén waves or modified Alfvén waves; cf. Arons & Barnard 1986).

For the subluminal waves, the dispersion equation (2) gives

$$\omega^2 = k_\varphi^2 c^2 \left(1 - \frac{k_z^2 c^2}{8\langle\gamma\rangle \omega_p^2}\right), \tag{5}$$

$$\langle\gamma\rangle = \int dp_\varphi \gamma f \tag{6}$$

(Machabeli 1991), provided that the conditions

$$1 - \frac{\omega}{k_\varphi c} \ll \tfrac{1}{2}\gamma_0^{-2}, \qquad \gamma_0 \equiv \langle\gamma^{-3}\rangle^{-1/4} \langle\gamma\rangle^{1/4} \tag{7}$$

and

$$4\langle\gamma\rangle \left(\frac{\omega_p}{\omega}\right)^2 \gg 1 \tag{8}$$

are satisfied. Condition (7) is valid provided that the refractive index approaches unity for small angles θ. Condition (8) requires that the Lorentz factor of the pair plasma be not too small and that the pair plasma be sufficiently dense.

When the Lorentz factor of the pair plasma is relatively large, the condition

$$\tfrac{1}{2}\gamma_0^{-2} < |1 - n_\varphi| \ll \langle\gamma^{-3}\rangle^{1/2} \left(\frac{\omega_p}{\omega}\right) \tag{9}$$

can be satisfied. For waves with a refractive index close to unity, one has the condition

$$\omega \gg \langle\gamma^{-3}\rangle^{1/2} \omega_p. \tag{10}$$

Inequality (9) also implies

$$\tfrac{1}{2}\gamma_0^{-2} \ll \langle\gamma^{-3}\rangle^{1/2} \left(\frac{\omega_p}{\omega}\right), \tag{11}$$

which reduces to (8), i.e. $\omega \ll 2\langle\gamma\rangle^{1/2}\omega_p$. With conditions (10) and (8), one has the dispersion equation

$$1 - n_\varphi = -\frac{2\omega_p^2}{\omega^2 n_z^2} \langle\gamma^{-3}\rangle, \tag{12}$$

with $n_z = k_z c/\omega$. Condition (10) requires that n_z satisfy

$$n_z^2 \gg \frac{2\omega_p^2}{\omega^2} \langle\gamma^{-3}\rangle. \tag{13}$$

For the case relevant to pulsars, we also require $n_z^2 < 1$. When there is no curvature drift effect, the waves described by the dispersion equation (12) cannot be excited. Since $\gamma_0 < \gamma_b$ and $|1 - n_\varphi| > \gamma_0^{-2}/2 > \gamma_b^{-2}/2$, the resonance condition $\omega - k_\varphi v_\varphi^b = 0$ (with v_φ^b the beam-particle velocity along the field line) cannot be satisfied without curvature drift.

From equations (2) and (5), when $\boldsymbol{k}$ is along the magnetic field line, the electrostatic transverse waves split into two types. The first type is tranverse, with a refractive index equal to unity and the electric field in the $\boldsymbol{e}_z$ direction. In this case, superposition of polarization in the $\boldsymbol{e}_z$ and $\boldsymbol{e}_r$ directions (the latter is determined by equation 1) can result in circular or elliptical polarization. The second type of wave is a Langmuir wave, which is discussed in Section 4.

3 INSTABILITY DRIVEN BY CURVATURE DRIFT

Earlier investigations of possible instabilities of the beam–plasma system in a pulsar magnetosphere were mainly based on the assumption that the pair plasma is uniformly magnetized (for a review see Lominadze et al. 1986). In a model in which the pair plasma is taken as a uniformly magnetized plasma and the cyclotron effect is neglected, the only possible instability is that for longitudinal waves (propagating along the field lines). When curvature drift is included, however, instability for the electrostatic transverse waves described by (5) and (12) can occur. Moreover, instability for longitudinal waves propagating along $\boldsymbol{B}$ is suppressed if the Lorentz factor of the beam is too large.

3.1 Amplified electrostatic transverse waves

In most pulsar magnetospheric models, the Lorentz factor of the primary particle beam is large (as large as $\gamma\approx 10^6$; e.g. Ruderman & Sutherland 1975; Arons 1981) and (3) can easily be satisfied. Curvature drift can therefore play an important role in the beam–plasma interaction in the sense that it can change the wave absorption properties. In this section we consider the beam–plasma instability driven by curvature drift. The response tensor can be written as $K_{\varphi\varphi}=1-\Delta K^{\rm p}_{\varphi\varphi}-\Delta K^{\rm b}_{\varphi\varphi}$, $K_{z\varphi}=-\Delta K^{\rm b}_{z\varphi}$ and $K_{zz}=1-\Delta K^{\rm b}_{zz}$, where $\Delta K^{\rm p}_{\varphi\varphi}$ and $\Delta K^{\rm b}_{ij}$ (with $i,j=\varphi,z$) represent the components of the main plasma and the beam, respectively. Consider the case of a cold beam. For subluminal waves, then, $\omega<k_\varphi c$, and when $|1-n_\varphi|\ll 1$ one has

$$\Delta K^{\rm b}_{\varphi\varphi}=\frac{\omega_{\rm b}^2\eta}{\gamma_{\rm b}^3\Omega_{\rm b}^2},\tag{14a}$$

$$\Delta K^{\rm b}_{z\varphi}=\frac{\omega_{\rm b}^2\theta_{\rm d}\eta}{\gamma_{\rm b}^3\Omega_{\rm b}^2},\tag{14b}$$

$$\Delta K^{\rm b}_{zz}=\frac{\omega_{\rm b}^2\theta_{\rm d}^2\eta}{\gamma_{\rm b}^3\Omega_{\rm b}^2}\tag{14c}$$

(Kazbegi et al. 1989; Luo 1993b), where near the resonance $[1-n_\varphi\approx\theta\theta_{\rm d}$; see (15)] one has $\eta\approx 1-\theta_{\rm d}^2\gamma_{\rm b}^2+\theta_{\rm d}\theta\gamma_{\rm b}^2$ (with $\gamma_{\rm b}$ the Lorentz factor of the beam particles), $\beta_{\rm d}=v_{\rm d}/c\approx\theta_{\rm d}$ and $\Omega_{\rm b}=\omega-k_\varphi c(1-\gamma^{-2}/2-\theta_{\rm d}^2/2)-k_z v_{\rm d}$. In the presence of curvature drift and when (3) is satisfied, the terms $\theta_{\rm d}^2\gamma_{\rm b}^2$ and $\theta\theta_{\rm d}\gamma_{\rm b}^2$ in (14a–c) can be important to the beam–plasma interaction.

Before estimating the growth rate, one first examines the resonance condition and specifies the angle at which the instability occurs. The resonance condition $\Omega_{\rm b}=0$ can be rewritten as

$$-\frac{n_\varphi^2 n_z^2}{\Delta K^{\rm p}_{\varphi\varphi}}+\tfrac{1}{2}n_\varphi(\gamma_{\rm b}^{-2}+\theta_{\rm d}^2)-\theta_{\rm d}\theta n_\varphi=0,\tag{15}$$

provided that (7) and (8) are satisfied. In the straight field line case, the Cerenkov condition can be satisfied simply by equating the velocity of the particles to the parallel phase velocity of the waves, where it is assumed that the particles move along the field lines. When the particles move along the drift orbit, the curvature drift term appears in the Cerenkov condition (15). Consider two cases: (a) $|k_z|/k\sim|\theta_{\rm d}|$, $\gamma_{\rm b}^{-1}$, and (b) $|k_z|/k\gg|\theta_{\rm d}|$, $\gamma_{\rm b}^{-1}$. In case (a), the resonance condition can be satisfied for either $k_z v_{\rm d}>0$ or $k_z v_{\rm d}<0$, with $n_\varphi^2 n_z^2/\Delta K^{\rm p}_{\varphi\varphi}+\theta_{\rm d}\theta n_\varphi>0$. One can show that the growth rate is negligible. In case (b), one may consider that $\theta_{\rm d}^2$ and $\gamma_{\rm b}^{-2}$ are of the same order of magnitude and $n_\varphi^2 n_z^2/\Delta K^{\rm p}_{\varphi\varphi}\gg\theta_{\rm d}^2$, $\gamma_{\rm b}^{-2}$. To satisfy the resonance condition, one must have $\theta_{\rm d}\theta<0$ to cancel the term $n_\varphi^2 n_z^2/\Delta K^{\rm p}_{\varphi\varphi}$. One then has

$$\theta_0\approx-\theta_{\rm d}\Delta K^{\rm p}_{\varphi\varphi}=-8\theta_{\rm d}\gamma_{\rm p}\left(\frac{\omega_{\rm p}}{\omega}\right)^2.\tag{16}$$

Thus the instability occurs at an angle $|\theta_0|\gg|\theta_{\rm d}|$. As a numerical example, for $\omega_{\rm p}=5\times10^{11}\ {\rm s}^{-1}$, $\omega=3\times10^{11}\ {\rm s}^{-1}$, $\gamma_{\rm p}=10^2$ and $\theta_{\rm d}\approx 3\times10^{-5}$, one has $\theta_0\approx-0.07$ which is much larger than the drift angle. The higher the frequency, the closer to the field line direction the instability occurs. This result is consistent with that derived in the rarefied plasma case, in which the maser emission is operative only at an angle much larger than the drift angle (LM).

To estimate the growth rate, one rewrites the frequency as $\omega+\Delta\omega$, with $\Delta\omega$ the frequency shift due to the presence of the beam. Here it is assumed that $|\Delta\omega|\ll\omega$. For illustrative purposes it is also assumed that the background plasma is cold with a Lorenz factor of $\gamma_{\rm p}$. The growth rate of the waves is then

$$\Gamma_{\rm a}=2|{\rm Im}\,\Delta\omega|.\tag{17}$$

The beam contributes significantly to the dispersion equation (2) only when $\Omega_{\rm b}=\Delta\omega$, i.e. when the beam particles have velocities satisfying the Cerenkov resonance condition. From (2) and (14a–c), using $\Omega_{\rm b}=\Delta\omega$, the growth rate is estimated to be

$$\Gamma_{\rm a}\approx 2\omega_{\rm b}|\theta_{\rm d}|\left(\frac{\gamma_{\rm p}}{\gamma_{\rm b}}\right)^{1/2}\left(\frac{\omega_{\rm p}}{\omega}\right),\tag{18}$$

provided that $k_z v_{\rm d}<0$ and $|\theta_{\rm d}|>1/\gamma_{\rm b}$. For $|\theta_{\rm d}|<1/\gamma_{\rm b}$, one finds that the growth rate is smaller than (18) by a factor of $|\theta_{\rm d}\gamma_{\rm b}|<1$. Fig. 1 shows the dependence on k of the growth rate $\Gamma_{\rm a}$. The numerical calculation is based on finding the imaginary roots of the dispersion equation (2), including the contribution from an energetic beam of positrons. The figure displays a resonant feature, which corresponds to the Cerenkov resonance condition $\Omega_{\rm b}=0$. The curve is plotted with $\gamma_{\rm b}=10^6$, $\gamma_{\rm p}=10^2$, $\omega_{\rm p}=5\times10^{11}\ {\rm s}^{-1}$, $\omega_{\rm b}^2/\omega_{\rm p}^2=10^{-4}$, $k_z/k=-0.08$, $\omega_B=10^{14}\ {\rm s}^{-1}$ and $R_B=10^5$ m. With these parameters, from (18), the growth rate is estimated to be $\sim5\times10^3$, which is consistent with the numerical calculation given in Fig. 1.

Based on the full dispersion relation (Luo 1993b), the growth rates are calculated for different k_r/k. The results are listed in Table 1, which shows that the growth rate is not sensitive to the value of k_r as long as k_r is not too large. This implies that the wave amplification is determined only by the angle between the electric field vector and the field line plane. This is expected since the mechanism is a result of curvature drift, which is always in the direction perpendi-

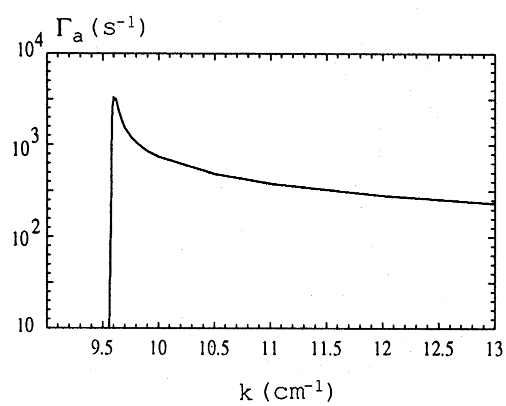

Figure 1. A plot of growth rate as a function of k for $|1-n_\varphi|\ll\gamma_0^{-2}/2$. The beam consists of positrons ($\theta_{\rm d}>0$). The curve displays a resonance at $k\approx 9.58\ {\rm cm}^{-1}$, which corresponds to the Cerenkov resonance condition $\Omega_{\rm b}=0$.

Table 1. The growth rates for different k_r ($\mathrm{cm^{-1}}$). The growth rates are derived with $\gamma_b=10^6$, $\gamma_p=10^3$, $\omega_p=10^{11}\ \mathrm{s^{-1}}$, $\omega_b^2/\omega_p^2=10^{-3}$, $k_z/k=-0.1$, $k=0.28\ \mathrm{cm^{-1}}$, $\omega_B=10^{14}\ \mathrm{s^{-1}}$ and $R_B=10^4$ m.

k_r ($\mathrm{cm^{-1}}$)	0	10^{-3}	10^{-2}	10^{-1}
Γ_a ($\mathrm{s^{-1}}$)	6.89×10^3	6.89×10^3	7.92×10^3	0.926×10^3

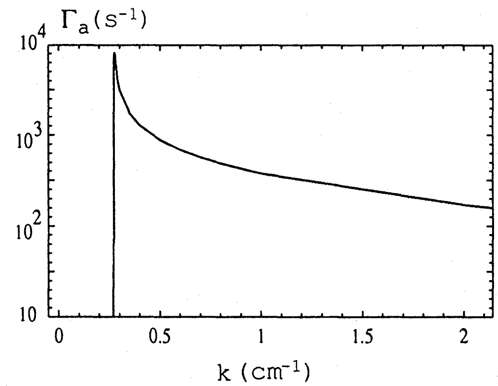

Figure 2. A plot of growth rate versus k for $|1-n_\varphi|>\gamma_0^{-2}/2$. The Cerenkov resonance condition corresponds to $k\approx0.28\ \mathrm{cm^{-1}}$.

cular to the field line plane, and the resonance condition is dependent on θ rather than on the azimuthal angle ϕ of $\boldsymbol{k}$. This result is correct only when the field line is locally circular and $B=|\boldsymbol{B}|$ is treated as being locally constant.

When the Lorentz factor of the background plasma is large, the dispersion equation for the electrostatic transverse waves reduces to (12). Following an argument similar to that leading to (16), by assuming $|k_z/k|\gg|\theta_d|$, γ_b^{-1}, one finds that the instability occurs at the angle defined by

$$\theta_0\approx-\frac{2^{1/3}}{\gamma_p|\theta_d|^{1/3}}\left(\frac{\omega_p}{\omega}\right)^{2/3}\left(\frac{\theta_d}{|\theta_d|}\right). \tag{19}$$

This angle has a weaker dependence on frequency than does (16). For a positron beam, the instability occurs at an angle $\theta_0<0$, with $|\theta_0|\gg\theta_d>0$. For an electron beam, one has $\theta_d<0$ and the instability occurs at an angle $\theta_0>0$. For either an electron beam or a positron beam, the growth rate is estimated to be

$$\Gamma_a=2^{2/3}\frac{\omega_b}{\sqrt{\gamma_p\gamma_b}}\left(\frac{\omega_p}{\omega}\right)^{1/3}|\theta_d|^{1/3}, \tag{20}$$

provided that $|\theta_d|>1/\gamma_b$. For $|\theta_d|<1/\gamma_b$, the growth rate is smaller than (20) by $|\theta_d|\gamma_b/4<1$. Fig. 2 shows a plot of growth rate as a function of wavenumber k with $\gamma_b=10^6$, $\gamma_p=10^3$, $\omega_p=10^{11}\ \mathrm{s^{-1}}$, $\omega_b^2/\omega_p^2=10^{-3}$, $k_z/k=-0.1$, $k_r/k=0$, $\omega_B=10^{14}\ \mathrm{s^{-1}}$ and $R_B=10^4$ m. As an example we assume that the beam is composed of positrons, $\theta_d>0$. Here both Γ_a and θ_0 are less dependent on the frequency ω than they are in (16) and (18).

3.2 The infinite magnetic field limit

From the preceding discussion, instability is not possible in the infinite magnetic field limit. When $B\to\infty$ the curvature drift disappears and the growth rates (18) and (20) vanish. This is consistent with the maser theory presented by LM, and is also consistent with the results given by APS. BGI, however, proposed a theory of curvature maser emission based on the assumption that wave amplification can occur for a plasma in a curved field line under a strong field limit driven by intrinsic field line curvature. The growth rate found by BGI appears to be inconsistent with the results found here. In LM, and in Section 3.1, it is shown that for the cases of both rarefied and dense plasma the existence of instability relies on the curvature drift, with the presence of free energy in the form of an inverted particle distribution also being essential. In the infinitely strong magnetic field limit, the curvature drift vanishes and there is no transverse motion. The response tensor has only a parallel component $K_{\varphi\varphi}$ since the particles only slide along the magnetic field lines. BGI's model based on this assumption led them to conclude that, even for a wave vector parallel to the field line direction, the electric field of the electrostatic transverse waves (they called them curvature plasma waves) has a non-zero component along the field line and that wave excitation in this case is possible. BGI's result appears to contradict what one may expect from the familiar case of curvature emission, in which the beaming approximation (obtained by assuming that the time-scale of the interaction between particles and waves is small compared with $1/\omega_R$, where $\omega_R\approx c/R_B$) is used. From the curvature emission formula (Luo 1993b), when $\boldsymbol{k}$ is along the field line (without twisting) and there is no curvature drift, there is no radiation with an electric field perpendicular to the field line plane. Thus it is hardly conceivable that, for particles streaming homogeneously along *circular* field lines, waves with an electric field perpendicular to the field line plane can be excited by a perturbation of the particle motion along the field line. Machabeli (1991) showed that in this case the lowest order interaction (via Cerenkov resonance) between the particle and the waves with the electric field being perpendicular to the field line is ineffective and wave amplification is not possible (Blandford 1975; Melrose 1978).

BGI's model appears to be inconsistent with the standard geometrical optics approximation (see Appendix A), as pointed out by Nambu (1989). The geometrical optics approximation is appropriate when the wavelength is small compared with the characteristic lengthscale of the inhomogeneity. The response tensor can be approximated by $K_{ij}\approx K_{ij}^{(0)}(\boldsymbol{k},\omega,\boldsymbol{x},t)+K_{ij}^{(1)}(\boldsymbol{k},\omega,\boldsymbol{x},t)$, where $K_{ij}^{(1)}$ is the λ/R_B correction (cf. equations A2 and A12). The first term $K_{ij}^{(0)}(\boldsymbol{k},\omega,\boldsymbol{x},t)$ can be derived in the local approximation (Krall & Trivelpiece 1973, p. 425), i.e. by assuming that the perturbed field and distribution vary locally as $\exp[-\mathrm{i}(\omega t-\boldsymbol{k}\cdot\boldsymbol{x})]$, with the amplitudes being treated as being locally constant. Only using this assumption can one obtain the dispersion relation in the general form given by equations (1) and (2). From (A14) and (A15a–c), the growth or damping is determined by $K_{ij}^{(0)}$, and the λ/R_B correction only changes the ray trajectory.

Finally, in BGI's model it appears that there is no free energy source, whereas one is needed to sustain any instability. In the maser theory presented by LM and Luo (1993a), the source of free energy corresponds to the requirement of an effective inversion of the particle population in the form $df(\gamma)/d\gamma>0$. In the beam–plasma instability the free energy is supplied by the kinetic energy of the beam particles, and is transformed into wave energy via the resonance interaction. In BGI's model, there is no beam and no requirement for an effective inversion of the particle population.

4 CURVATURE DRIFT EFFECT ON LANGMUIR WAVE INSTABILITY

The dispersion relation (2) allows the existence of Langmuir waves propagating in the field line direction provided that the curvature drift for the background plasma is negligible, $|\theta_d^p|\ll 1$. The dispersion equation for this type of wave can be approximated by

$$1-\Delta K^p_{\varphi\varphi}=0, \tag{21}$$

where $\Delta K^p_{\varphi\varphi}=1-K_{\varphi\varphi}$ is given by (4) with $\theta=0$. It is well known that, for straight field lines, an instability can develop for Langmuir waves with $|1-n|\ll 1$, due to the Cerenkov resonance interaction of the beam particles and waves (Egorenkov, Lominadze & Mamradze 1983). One interesting question is how the curvature drift modifies such an instability when the Lorentz factor of the beam particles is large. Before going into a detailed discussion, consider the Langmuir wave instability in the case of straight field lines.

For straight field lines, the dispersion relation modified by a beam with $\Omega_b=\Delta\omega$ (the beam particles are approximately in resonance with the waves) reads

$$1-\Delta K^p_{\varphi\varphi}-\frac{A}{(\Delta\omega)^2}=0, \tag{22}$$

with

$$A=\frac{\omega_b^2}{\gamma^3}, \tag{23}$$

where $\Delta K^p_{\varphi\varphi}$, the relevant contribution from the dense pair plasma, is given by

$$\Delta K^p_{\varphi\varphi}=4\frac{\omega_p^2}{k_\varphi^2c^2}\left(\langle\gamma\rangle-\frac{4\Delta\omega\langle\gamma^3\rangle}{k_\varphi c}\right), \tag{24}$$

provided that $|\Delta\omega/k_\varphi c|\ll 1$. When the second of the terms within the brackets on the right-hand side of (24) is neglected, (22) gives

$$\Delta\omega^2=\frac{A}{1-\Delta K^p_{\varphi\varphi}}. \tag{25}$$

Since A given by (23) is always positive and $|\Delta K^p_{\varphi\varphi}|\gg 1$, the instability can occur with a growth rate given by

$$\Gamma_a=2\left(\frac{\omega_b}{\omega_p}\right)\frac{k_\varphi c}{\gamma_b^{3/2}\langle\gamma\rangle^{1/2}} \tag{26}$$

(Egorenkov et al. 1983). When the second of the terms within the brackets on the right-hand side of (24) is important, one finds the growth rate

$$\Gamma_a=\frac{3^{1/2}}{2}\left(\frac{\omega_b}{\omega_p}\right)\frac{k_\varphi c}{\gamma_b\langle\gamma^3\rangle^{1/3}} \tag{27}$$

(Egorenkov et al. 1983). When curvature drift is taken into account, and when the beam particles have a large Lorentz factor, the instability described by (26) and (27) tends to be suppressed, either due to a significant contribution to the dispersion from the off-diagonal curvature drift terms in (2) or because (23), after modification by a curvature drift term, can be negative. The condition for the instability to be completely suppressed in the latter case can be derived as follows. When curvature drift is important, and since in (14a) $\eta\approx 1-\theta_d^2\gamma_b^2$, A in (23) may be modified as

$$A=\frac{\omega_b^2}{\gamma^3}(1-\gamma_b^2\theta_d^2), \tag{28}$$

which can be negative for $\gamma_b^2\theta_d^2>1$. Thus the condition for positive A is that the Lorentz factor must satisfy $\gamma_b^2\theta_d^2<1$, which can be rewritten as

$$\gamma_b<2.3\times 10^5\left(\frac{B}{10^4\ \mathrm{T}}\right)^{1/2}\left(\frac{R_B}{10^4\ \mathrm{m}}\right)^{1/2}. \tag{29}$$

Equation (29) then imposes an upper limit on γ_b of the beam for the instability to occur. For some pulsar magnetospheric models with a large Lorentz factor for the beam particles (e.g. Beskin, Gurevich & Istomin 1983) the instabilities described by (26) and (27) may not develop and can be completely suppressed by curvature drift. For electrostatic waves with $\boldsymbol{k}=k_\varphi\boldsymbol{e}_\varphi$, the electric field vector is in the $\boldsymbol{e}_\varphi$ direction and instability can occur when the velocities of the particles of the fast component (beam) of the plasma satisfy the Cerenkov resonance condition. In the one-dimensional case, in the wave frame, this instability is attributed to the fast particles (with velocities approximately equal to the Cerenkov resonance) bunching around the stationary phase point. When the Lorentz factor of the particles of the beam is large, the curvature drift velocity (across the field line) is also large and the particles cannot fully interact with waves before they drift out of the interaction region. The actual value of the upper limit is explicitly dependent on the distance from the stellar surface. For a dipolar field, the radius of curvature is about $R_B\gtrsim 2(rc/\Omega)^{1/2}$, with Ω the angular velocity of the neutron star. From (29) one then finds that the instability can occur only at an altitude lower than

$$r<8.9\times 10^5\left(\frac{P}{1\ \mathrm{s}}\right)^{1/5}\left(\frac{B_s}{10^8\ \mathrm{T}}\right)^{2/5}\left(\frac{10^6}{\gamma_b}\right)^{4/5}\ \mathrm{m}, \tag{30}$$

where P and B_s are the period and the surface magnetic field of a pulsar. For Ruderman & Sutherland's (1975) model, in which $B_s=10^8$ T and $P=1$ s, the instability can occur only within the distance $r<8.9\times 10^5$ m. For the Crab pulsar, for which $P=33$ ms and $B_s=10^4$ T, this distance is estimated to be $r<10^4$ m. Thus there is a serious constraint on the applicability of an emission model that relies on a longitudinal wave instability produced by an energetic beam.

5 APPLICATION TO RADIO PULSARS

The essential feature of the coherent theory developed here is that it requires an energetic beam. The minimum Lorentz factor required for curvature drift to play a role in the wave–plasma interaction is $\gamma_c=1/|\theta_d\Delta\theta_0|^{1/2}>1/|\theta_d|^{1/2}$. In practice, since the contribution to the plasma dispersion from the beam is proportional to $\theta\theta_d\gamma_b^2$, to obtain a sufficient growth rate (cf. equations 14a–c) the Lorentz factor of the beam particles needs to satisfy $\gamma \gg \gamma_c$. The smallest value of γ_c is about 10^4. Hence the energetic beam can be identified as the primary beam or another charge-separated beam that is accelerated in the gap (e.g. Arons 1981). In most presently available gap models, such as Arons's (1981) slot gap model, the energy of the beam particles acquired from the gap acceleration is more than enough to account for the radio emission. This is because the energy invested in radio emission is always a small fraction of the overall energy budget (Manchester & Taylor 1977).

The most important constraints on any proposed instability mechanism for pulsar radio emission are that the plasma instability occurs well within the light cylinder, and that the mechanism can at least qualitatively explain the main features of observed spectra and polarization. Since the actual value of the growth rate is dependent on the details of the plasma conditions, which are not well understood, here only the necessary condition for the instability to develop is considered. This condition corresponds to the e-folding distance of the growth being much smaller than the distance to the light cylinder. In this paper, although no attempt is made to give a complete radio emission model, it is suggested that due to curvature drift the instability for electrostatic transverse waves can occur well within the light cylinder, and that this may be responsible for the pulsar radio emission. The growth rates given by (18) and (20) can be rewritten as

$$\Gamma_a \approx 10^4\left(\frac{N_b}{10^{16}\ \mathrm{m}^{-3}}\right)\left(\frac{R_B}{10^5\ \mathrm{m}}\right)^{-1}\left(\frac{B}{10^4\ \mathrm{T}}\right)^{-1} \times\left(\frac{\gamma_b}{10^6}\right)\left(\frac{\omega}{10^{10}\ \mathrm{s}^{-1}}\right)^{-1}\ \mathrm{s}^{-1} \qquad (31)$$

and

$$\Gamma_a \approx 78(2\delta)^{2/3}\left(\frac{N_b}{10^{16}\ \mathrm{m}^{-3}}\right)^{2/3}\left(\frac{R_B}{10^5\ \mathrm{m}}\right)^{-1/3} \times\left(\frac{B}{10^4\ \mathrm{T}}\right)^{-1/3}\left(\frac{\gamma_b}{10^6}\right)^{-2/3}\left(\frac{\omega}{10^{10}\ \mathrm{s}^{-1}}\right)^{-1/3}\ \mathrm{s}^{-1}, \qquad (32)$$

where an energy equipartition between the beam and the background plasma $\gamma_p N_p \approx \gamma_b N_b$ is assumed, and where $\delta = N_p/N_b \approx \gamma_b/\gamma_p$. For $B = 10^4$ T, $R_B = 10^5$ m, $N_b = 10^{16}\ \mathrm{m}^{-3}$, $\gamma_b = 10^6$, $\delta \approx 10^3$ and $\omega = 10^{10}\ \mathrm{s}^{-1}$, using (31) or (32), one has $\Gamma_a/\Omega > \Gamma_a/\omega_R > 1$ (with $R_B < R_L$), which implies that in principle the instability can occur within the light cylinder (the e-folding distance is about 3×10^4 m, whereas for a typical pulsar the distance to the light cylinder is about $R_L \sim 10^7$ m). To obtain a large enough growth rate one must use large N_b. To compare with the growth rate of the curvature maser emission, one may rewrite the growth rate (18) as $\Gamma_a \approx 2\sqrt{2}(\tilde{\omega}_B/\omega)(W_p/W_m)\gamma_b\omega_R$, which is much larger than the growth rate $\Gamma_a \approx (1/4\pi)(\tilde{\omega}_B/\omega)(W_p/W_m)\omega_R$ found in LM for the larger negative absorption peak (at $\theta \approx \pm\Delta\theta_0$) in the maser emission case. In contrast to the maser emission mechanism (LM), therefore, the 'hydrodynamic' instability discussed here does not seem to exclude millisecond pulsars with $B \sim 10^4$ T.

The emission mechanism discussed here is narrow-band, as expected since the instability is due to a resonant interaction. The intrinsically narrow-band emission may result in broad-band emission, as observed, if there is (a) broadening due to variation in the density along the altitude, or (b) broadening due to variation in the density in the direction perpendicular to the rotation axis. In the former case, since the plasma streaming is along the field lines and the magnetic field B decreases as the distance to the star increases according to $B \sim r^{-3}$ for a dipolar field, the plasma density falls in the same way as the magnetic field. The resonance condition is sensitive to the plasma density, which strongly depends, as r^{-3}, on the distance from the surface of the star, and is also sensitive to the radius of curvature. The broad-band observed emission can be attributed to radiation from different sources at different altitudes. The broadening due to variation in the density in the direction perpendicular to the rotation axis was discussed by APS.

An instability occurs for waves propagating at a small angle to the field line. The angle can be estimated by (16) or (19). Fig. 3 shows how the growth rate depends on the angle θ. The angular width (the so-called 'perpendicular wavenumber window') within which the instability has a significant growth rate (corresponding to the half-peak width) is about a few per cent of a degree.

The frequency of the amplified electrostatic transverse waves has upper and lower cut-off frequencies. The upper cut-off frequency is given by $\omega \ll \omega_{\max} = 2\langle\gamma\rangle^{1/2}\omega_p$ (cf. equation 8). The lower cut-off frequency $\omega_{\min}$ can be derived by applying the condition $|\theta| < 1$ to (16) (the instability occurs at a small angle to the field line). Using $|\theta| \approx |\theta_d|\Delta K^p_{\varphi\varphi} < 1$, one has $\omega > \omega_{\min} = 2|\theta_d|^{1/2}\omega_p\gamma_p^{1/2}$. The upper and lower cut-off frequencies depend explicitly on both the density and the radius of curvature; hence they depend on the location of the emission zone. As the altitude increases, $\omega_{\max}$ and $\omega_{\min}$ shift towards lower frequencies, which implies that a source region at a lower altitude generates higher frequency radiation. This is consistent with the overall radius–frequency map obtained from observations (Blaskiewicz, Cordes & Wasserman 1991) using the relation of pulse width to frequency. The pulse width depends on the geometry of the field lines and on the detailed emission mechanism. If one assumes that radiation is generated in the region confined to the diverging cone of the dipolar field lines, the angular

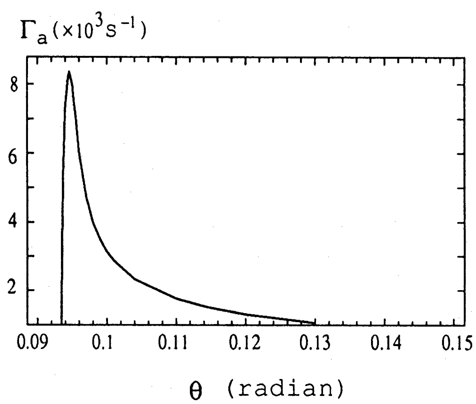

Figure 3. The growth rate as a function of viewing angle θ (in radians). In the figure, $\omega_p = 10^{11}\ \mathrm{s}^{-1}$, $\gamma_b = 10^6$, $N_b/N_p = 10^{-3}$, $R_B = 10^4$ m and $k = 0.3\ \mathrm{cm}^{-1}$. The energetic beam is composed of electrons.

spread at a given radial distance r from the surface is given by $\theta_\omega \approx (3/2)(\Omega r/c)^{1/2}$. The observed angular width d_ω varies with frequency ω approximately as $d_\omega \propto \omega^p$ (Manchester & Taylor 1977; Smith 1991), where p ranges from -0.2 to -0.5. If $p=-0.25$, one can infer the relation $r \propto \omega^{-0.5}$. Since the resonances depend on both frequency and the angle θ, one cannot specify a particular frequency. Nevertheless, one can estimate the radius-to-$\omega_{\max}$ (or $\omega_{\min}$) mapping from the point of view of the emission mechanism itself. For the upper cut-off frequency, $\omega_{\max} \sim r^{-3/2}$, one has $r \propto \omega_{\max}^{-0.67}$. Here a dipolar field is assumed and hence the plasma density falls off in the same way as the magnetic field as the altitude increases (since the plasma flows along the field lines). If one takes $\omega \sim \omega_{\min}$, the scaling of the emission radius with frequency is much stronger than $r \propto \omega^{-0.5}$. When the background plasma is relatively energetic, the dispersion equation (12) is appropriate, and its lower cut-off frequency is given by

$$\omega \gtrsim \omega_{\min} = \frac{\sqrt{2}}{\gamma_p^{3/2} |\theta_d|^{1/2}}\, \omega_p. \tag{33}$$

Assuming a dipolar field and the constant γ_p, for $\omega \sim \omega_{\min}$ the emission radius scales with frequency as $\omega^{-0.36}$, which agrees with observation (Blaskiewicz et al. 1991).

The mechanism discussed here is predominantly linearly polarized. Let E_φ and E_z be the perturbed electric fields along the φ- and z-components, respectively. From the wave equation, since $\Delta K^p_{\varphi\varphi} \gg 1$, one has

$$\left|\frac{E_\varphi}{E_z}\right| \approx \frac{|n_z|\, n_\varphi}{\Delta K^p_{\varphi\varphi}} \ll 1. \tag{34}$$

This corresponds to linear polarization with an electric field approximately perpendicular to the projection of the field line on the plane of the sky. This can provide a natural explanation of the position angle swing in observed pulses. One may define the position angle in the same way as for curvature emission, i.e. one can define the position angle in terms of the projected magnetic field line. The mechanism of electrostatic transverse wave instability itself cannot provide circular polarization. To account for the circular polarization observed in some pulsars, one must appeal to other mechanisms that take into account, for example, the effect of cyclotron resonance (Kazbegi, Machabeli & Melikidze 1991) or the effect of the birefringence of the background plasma (cf. Melrose & Stoneham 1977; Melrose 1979).

6 CONCLUSIONS AND DISCUSSION

In this paper we consider instabilities in a model pulsar magnetosphere in which the plasma is composed of a highly relativistic ($\gamma_b \gtrsim 10^5$) beam moving through a relativistic ($\gamma_p \approx 10^2$–10^3) pair plasma. Emphasis is placed on the role of curvature drift, $v_d = c^2 \gamma_b / \omega_B R_B$, which is an essential ingredient of maser curvature emission. The main results of the investigation presented in this paper are as follows.

(i) The drift velocity of the primary beam can lead to a hydrodynamic-type instability of the so-called electrostatic transverse waves. Since the electrostatic transverse waves have an electromagnetic component, the waves can be excited and radiate directly. The maximum growth rate for the electrostatic transverse waves considered here occurs at an angle to the field line $|\theta| \gg |\theta_d|$, whereas in the case of the electrostatic instability discussed by APS the maximum growth rate occurs in the field line direction, at $\theta \approx 0$.

(ii) This instability does not exist in the limit $B \to \infty$, seemingly conflicting with the results of BGI, who found instability in this limit. The crucial point of the theory discussed here is the curvature drift effect. In the limit $B \to \infty$, there is no curvature drift and the growth rates (18) and (20) are zero.

(iii) This curvature drift effect tends to suppress instability of Langmuir waves due to the primary beam. Shaposhnikov (1981) studied the possible amplification of Langmuir waves by the curvature drift mechanism and suggested that curvature drift, under certain conditions, can enhance the Langmuir instability. In his treatment, the plasma dispersion was not taken into account. Kazbegi, Machabeli & Melikidze (1986) re-examined this problem by considering particles moving along circular field lines without curvature drift. They suggested that the intrinsic curvature cannot lead to significant enhancement of the instability. Kazbegi et al.'s (1986) result did not include curvature drift and, as a consequence, is inconclusive as to whether curvature drift is effective in driving the Langmuir wave instability.

(iv) The emission mechanism discussed here is narrowband. A broad-band spectrum can be obtained by assuming that the radiation is generated at different locations along the field line. A broad-band spectrum can also result from variation in the plasma density in the direction transverse to the rotation axis (for a detailed discussion, see APS).

(v) The lower and upper cut-off frequencies explicitly depend on the plasma density and the radius of curvature, and hence depend on the altitude. This implies a radius–frequency relation, with the higher frequency radiation generated at a lower altitude and the lower frequency radiation at a higher altitude, which is consistent with observation. The growth rate is proportional to the radial distance to the star. As the altitude increases the growth rate also increases. This suggests that the intensity will increase with decreasing frequency.

(vi) The emission mechanism itself produces linear polarization. The plasma instability theory presented here is in the linear regime. As a result of instability, large-amplitude waves can be produced. There is a critical value of the wave amplitude, above which the variation of the zeroth-order orbit of the particles becomes important and the energy transfer between the beam particles and the waves becomes oscillatory. A theory including non-linear effects is beyond the scope of this paper and is not discussed any further here.

ACKNOWLEDGMENTS

QL acknowledges the receipt of a Chinese Government Postgraduate Research Award and a Scholarship from the Research Centre for Theoretical Astrophysics.

REFERENCES

Arons J., 1981, in Sieber W., Wielebinski R., eds, IAU Symp. 95, Pulsars. Reidel, Dordrecht, p. 69
Arons J., Barnard J. J., 1986, ApJ, 302, 120
Asseo E., Pellat R., Sol H., 1983, ApJ, 266, 201 (APS)
Asseo E., Pellat R., Sol H., 1990, MNRAS, 247, 529
Bernstein I., Friedland L., 1983, in Galeev A. A., Sudan R. N., eds, Handbook of Plasma Physics, Vol. 1. North-Holland, Amsterdam, p. 367

Beskin V. S., Gurevich A. V., Istomin Ya. N., 1983, Sov. Phys. JETP, 58, 235
Beskin V. S., Gurevich A. V., Istomin Ya. N., 1988, Ap&SS, 146, 205 (BGI)
Blandford R. D., 1975, MNRAS, 170, 551
Blaskiewicz M., Cordes J. M., Wasserman I., 1991, ApJ, 370, 643
Cheng A. F., Ruderman M., 1977, ApJ, 212, 800
Chugunov Yu. V., Shaposhnikov V. E., 1988, Afz, 28, 98
Coppi B., Rosenbluth M. N., Sudan R. N., 1969, Ann. Phys., 55, 207
Egorenkov V. D., Lominadze D. G., Mamradze P. G., 1983, Afz, 19, 753
Kazbegi A. Z., Machabeli G. Z., Melikidze G. I., 1986, Afz, 25, 119
Kazbegi A. Z., Machabeli G. Z., Melikidze G. I., Usov V. V., 1989, Proc. Joint Varenna–Abastumani International School Workshop on Plasma Astrophys., Vol. 1. ESA Sp-285, ESA Publications Division, Noordwijk, p. 271
Kazbegi A. Z., Machabeli G. Z., Melikidze G. I., 1991, MNRAS, 253, 377
Kirk J. G., 1980, Plasma Phys., 22, 639
Krall N. A., Trivelpiece A. V., 1973, Principles of Plasma Physics. McGraw-Hill, New York
Larroche O., Pellat R., 1987, Phys. Rev. Lett., 59, 1104
Lominadze Dzh. G., Machabeli G. Z., Melikidze G. I., Pataraya A. D., 1986, Sov. J. Plasma Phys., 12, 712
Luo Q., 1993a, Proc. Astron. Soc. Aust., 10, 258
Luo Q., 1993b, PhD thesis, University of Sydney
Luo Q., Melrose D. B., 1992a, Proc. Astron. Soc. Aust., 10, 45
Luo Q., Melrose D. B., 1992b, MNRAS, 258, 616 (LM)
Machabeli G. Z., 1991, Plasma Phys. Contr. Fusion, 33, 1227
Manchester R. N., Taylor J. H., 1977, Pulsars. Freeman and Company, San Francisco
Manheimer W. M., Lashmore-Davies C. N., 1989, MHD and micro-instabilities in confined plasma. Adam Hilger, New York
Melrose D. B., 1978, ApJ, 225, 557
Melrose D. B., 1979, Aust. J. Phys., 32, 61
Melrose D. B., 1980, Plasma Astrophysics. Gordon & Breach, New York, Vols 1, 2
Melrose D. B., 1986, Instabilities in Space and Laboratory Plasma. Cambridge Univ. Press, Cambridge
Melrose D. B., Stoneham R. J., 1977, Proc. Astron. Soc. Aust., 3, 120
Nambu M., 1989, Plasma Phys. Contr. Fusion, 31, 143
Rowe E. T., 1992, Aust. J. Phys., 45, 21
Ruderman M. A., Sutherland P. G., 1975, ApJ, 196, 51
Shaposhnikov V. Z., 1981, Afz, 17, 749
Smith F. G., 1991, Comm. Astrophys., 15, 207
Sturrock P. A., 1971, ApJ, 164, 529
Sturrock P. A., Petrosian V., Turk J. S., 1975, ApJ, 196, 73
Usov V. V., 1987, ApJ, 320, 333
Zheleznyakov V. V., Shaposhnikov V. E., 1979, Aust. J. Phys., 32, 49

APPENDIX A: GEOMETRICAL OPTICS APPROXIMATION

A1 Induced current

For a weakly non-stationary and inhomogeneous plasma the induced current is given by

$$J_i(\boldsymbol{x}, t) = \int \mathrm{d}\boldsymbol{x}' \int_{-\infty}^{t} \mathrm{d}t' \times \sigma[\boldsymbol{x}-\boldsymbol{x}', t-t'; \tfrac{1}{2}(\boldsymbol{x}+\boldsymbol{x}'), \tfrac{1}{2}(t+t')]_{ij} E_j(\boldsymbol{x}', t') \qquad \text{(A1)}$$

(Bernstein & Friedland 1983; Manheimer & Lashmore-Davies 1989, p. 279), where the first pair of variables gives the spatial and temporal dispersion dependences, and the second pair represents the weak dependence on the mean position and time variables due to the non-stationarity and inhomogeneity of the plasma. Let ξ be any scalar characterizing the background plasma, such as density, temperature, etc. ξ is said to be 'slowly varying' when the fractional change in ξ at a local wavelength $2\pi/k$ or local frequency $2\pi/\omega$ is small. Setting $\boldsymbol{\eta}=\boldsymbol{x}-\boldsymbol{x}'$ and $\tau=t-t'$, the conductivity tensor σ can be expanded as

$$\sigma_{ij}[\boldsymbol{x}-\boldsymbol{x}', t-t'; \tfrac{1}{2}(\boldsymbol{x}+\boldsymbol{x}'), \tfrac{1}{2}(t+t')] = \sigma_{ij}(\boldsymbol{\eta}, \tau; \boldsymbol{x}-\boldsymbol{\eta}/2, t-\tau/2) = \sum_{n=0}^{\infty} \frac{1}{n!}\left(-\tfrac{1}{2}\boldsymbol{\eta}\cdot\frac{\partial}{\partial \boldsymbol{x}} - \tfrac{1}{2}\tau\frac{\partial}{\partial t}\right)^n \sigma_{ij}(\boldsymbol{\eta}, \tau; \boldsymbol{x}, t). \qquad \text{(A2)}$$

For a non-stationary and inhomogeneous plasma, we consider the eikonal approximation

$$\boldsymbol{E}(\boldsymbol{x}, t) = \boldsymbol{\mathscr{E}}(\boldsymbol{x}, t)\exp[\mathrm{i}\psi(\boldsymbol{x}, t)],$$

where $\boldsymbol{\mathscr{E}}(\boldsymbol{x}, t)$ is a function that weakly depends on $\boldsymbol{x}$ and t and $\psi(\boldsymbol{x}, t)$ is a real function. A Taylor expansion yields

$$\psi(\boldsymbol{x}', t') = \psi(\boldsymbol{x}, t) - \boldsymbol{k}\cdot\boldsymbol{\eta} + \omega\tau + \tfrac{1}{2}\boldsymbol{\eta}\cdot\frac{\partial \boldsymbol{k}}{\partial \boldsymbol{x}}\cdot\boldsymbol{\eta} - \tfrac{1}{2}\tau^2\frac{\partial\omega}{\partial t} - \boldsymbol{\eta}\cdot\frac{\partial\omega}{\partial\boldsymbol{x}}\tau + \ldots \qquad \text{(A3)}$$

and

$$\boldsymbol{\mathscr{E}}(\boldsymbol{x}-\boldsymbol{\eta}, t-\tau) = \boldsymbol{\mathscr{E}}(\boldsymbol{x}, t) - \boldsymbol{\eta}\cdot\frac{\partial\boldsymbol{\mathscr{E}}}{\partial\boldsymbol{x}} - \tau\frac{\partial\boldsymbol{\mathscr{E}}}{\partial t} + \ldots, \qquad \text{(A4)}$$

where the wave vector and frequency are defined by $\boldsymbol{k}=\partial\psi/\partial\boldsymbol{x}$ and $\omega=-\partial\psi/\partial t$, which are slowly varying functions of $\boldsymbol{x}$ and t. The wave equation is given by

$$\nabla\times(\nabla\times\boldsymbol{E}) + \frac{1}{c^2}\frac{\partial^2\boldsymbol{E}}{\partial t^2} + \mu_0\frac{\partial\boldsymbol{J}}{\partial t} = 0. \qquad \text{(A5)}$$

Introduce $\sigma^{(0)}_{ij}$ by writing

$$\sigma^{(0)}_{ij}(\boldsymbol{k}, \omega; \boldsymbol{x}, t) = \int \frac{\mathrm{d}\boldsymbol{\eta}\,\mathrm{d}\tau}{(2\pi)^4}\sigma_{ij}(\boldsymbol{\eta}, \tau; \boldsymbol{x}, t)\exp[\mathrm{i}(\omega\tau - \boldsymbol{k}\cdot\boldsymbol{\eta})]. \qquad \text{(A6)}$$

The wave equation (A15) becomes

$$\left[\boldsymbol{I} + \frac{c^2}{\omega^2}(\boldsymbol{kk} - k^2\boldsymbol{I}) + \frac{i}{\varepsilon_0\omega}\sigma^{(0)}\right]\cdot\boldsymbol{\mathscr{E}} - \frac{c^2}{\omega^2}[\mathrm{i}\boldsymbol{k}\times(\nabla\times\boldsymbol{\mathscr{E}}) + \nabla\times(\mathrm{i}\boldsymbol{k}\times\boldsymbol{\mathscr{E}})] + \frac{1}{\omega^2}[\mathrm{i}\omega\partial_t\boldsymbol{\mathscr{E}} + \partial_t(\mathrm{i}\omega\boldsymbol{\mathscr{E}})] - \frac{1}{\varepsilon_0\omega^2}[\partial_t(\sigma^{(0)}\cdot\boldsymbol{\mathscr{E}}) - \mathrm{i}\omega\sigma^{(1)}\cdot\boldsymbol{\mathscr{E}}] = 0, \qquad \text{(A7)}$$

where $\partial_t = \partial/\partial t$ and $\nabla = \partial/\partial \boldsymbol{x}$, and where $\sigma^{(1)}_{ij}$ is defined by

$$\sigma^{(1)}_{lm} = -\frac{\mathrm{i}}{2}\nabla\cdot\left(\frac{\partial\sigma^{(0)}_{lm}}{\partial \boldsymbol{k}}\right) + \frac{\mathrm{i}}{2}\partial_t\left(\frac{\partial\sigma^{(0)}_{lm}}{\partial\omega}\right) - \mathrm{i}\frac{\partial\sigma^{(0)}_{lm}}{\partial k_j}\nabla_j + \mathrm{i}\frac{\partial\sigma^{(0)}_{lm}}{\partial\omega}\partial_t. \tag{A8}$$

The electric field is

$$\boldsymbol{\mathscr{E}} = \boldsymbol{\mathscr{E}}^{(0)} + \boldsymbol{\mathscr{E}}^{(1)} + \ldots, \tag{A9}$$

where $\boldsymbol{\mathscr{E}}^{(1)}$ and higher order terms are corrections due to non-stationarity and inhomogeneity.

A2 The wave kinetic equation

In order to determine which part of the permittivity is responsible for the dissipation of energy, one may start from the generalized dispersion relation

$$\int \mathrm{d}\boldsymbol{x}' \int \mathrm{d}t' \Lambda_{ij}[\boldsymbol{x}-\boldsymbol{x}', t-t'; \tfrac{1}{2}(\boldsymbol{x}+\boldsymbol{x}'), \tfrac{1}{2}(t+t')]\, E_j(\boldsymbol{x}', t') = 0, \tag{A10}$$

where Λ_{ij} is assumed to be a slowly varying function of $\boldsymbol{x}$ and t. For uniform plasma the equation, after Fourier transforming, reduces to

$$\Lambda_{ij}(\boldsymbol{k}, \omega)\,\mathscr{E}_j(\boldsymbol{k}, \omega) = 0, \tag{A11}$$

with

$$\Lambda_{ij} = (k^2c^2/\omega^2)(\hat{k}_i\hat{k}_j - \delta_{ij}) + K_{ij},$$

where $\hat{k}_i = k_i/k$, and $K_{ij} = \delta_{ij} + (\mathrm{i}/\varepsilon_0\omega)\,\sigma_{ij}$ is the equivalent dielectric tensor. Similarly to equation (A3), one has

$$\Lambda_{ij}[\boldsymbol{x}-\boldsymbol{x}', t-t'; \tfrac{1}{2}(\boldsymbol{x}+\boldsymbol{x}'), \tfrac{1}{2}(t+t')] = \Lambda_{ij}(\boldsymbol{\eta}, \tau; \boldsymbol{x}-\boldsymbol{\eta}/2, t-\tau/2)$$

$$= \sum_{n=0}^{\infty}\frac{1}{n!}\left(-\tfrac{1}{2}\boldsymbol{\eta}\cdot\frac{\partial}{\partial\boldsymbol{x}} - \tfrac{1}{2}\tau\frac{\partial}{\partial t}\right)^n \Lambda_{ij}(\boldsymbol{\eta}, \tau; \boldsymbol{x}, t). \tag{A12}$$

We also introduce $\Lambda_{ij}(\boldsymbol{k}, \omega; \boldsymbol{x}, t)$ by

$$\Lambda_{ij}(\boldsymbol{k}, \omega; \boldsymbol{x}, t) = \int \frac{\mathrm{d}\boldsymbol{\eta}\,\mathrm{d}\tau}{(2\pi)^4}\Lambda_{ij}(\boldsymbol{\eta}, \tau; \boldsymbol{x}, t)\exp[\mathrm{i}(\omega\tau - \boldsymbol{k}\cdot\boldsymbol{\eta})]. \tag{A13}$$

In the following discussion, the hermitian and antihermitian parts are denoted by $\Lambda^{\mathrm{H}}_{ij}$ and $\Lambda^{\mathrm{A}}_{ij}$, respectively. Substituting equations (A9), (A12) and (A13) into the wave equation (A10), and multiplying it by $\boldsymbol{\mathscr{E}}^*(\boldsymbol{x}, t)\exp[-\mathrm{i}\psi(\boldsymbol{x}, t)]$, one obtains

$$\left(\frac{\partial}{\partial t} + \frac{\partial\omega}{\partial\boldsymbol{k}}\cdot\frac{\partial}{\partial\boldsymbol{x}} - \frac{\partial}{\partial\boldsymbol{x}}\cdot\frac{\partial}{\partial\boldsymbol{k}}\right)N(\boldsymbol{x}, \boldsymbol{k}, t) = -\Gamma(\boldsymbol{k})\,N(\boldsymbol{x}, \boldsymbol{k}, t), \tag{A14}$$

where N, V and Γ are defined by

$$N = \frac{1}{4\pi\hbar}\mathscr{E}^*_i\mathscr{E}_j\frac{\partial\Lambda_{ij}}{\partial\omega}, \tag{A15a}$$

$$V = -\frac{\mathscr{E}^*_i\mathscr{E}_j\partial\Lambda^{\mathrm{H}}_{ij}/\partial\boldsymbol{k}}{\mathscr{E}^*_l\mathscr{E}_m\partial\Lambda^{\mathrm{H}}_{lm}/\partial\omega}, \tag{A15b}$$

$$\Gamma(\boldsymbol{k}) = -\frac{2\mathscr{E}^*_i\mathscr{E}_j\Lambda^{\mathrm{A}}_{ij}}{\mathscr{E}^*_l\mathscr{E}_m\partial\Lambda^{\mathrm{H}}_{lm}/\partial\omega}. \tag{A15c}$$

According to Bernstein & Friedland (1983), writing $\sigma^{(0)} = \sigma^{\mathrm{A}} + \sigma^{\mathrm{H}}$ and assuming $\sigma^{\mathrm{H}} \ll \sigma^{\mathrm{A}}$, one has

$$\Lambda^{(0)}_{ij} = \delta_{ij} + \frac{c^2}{\omega^2}(k_ik_j - k^2\delta_{ij}) + \frac{\mathrm{i}}{\varepsilon_0\omega}\sigma^{(0)}_{ij}. \tag{A16}$$

(A14) is then the wave kinetic equation, and N in (A15a) may be identified as the occupation number of wave quanta (Coppi, Rosenbluth & Sudan 1969; Manheimer & Lashmore-Davies 1989; Nambu 1989). The absorption coefficient Γ is given by

$$\Gamma(\boldsymbol{k}) = -2\mathrm{i}\omega R e^*_i e_j \Lambda^{\mathrm{A}}_{ij}, \tag{A17}$$

where R is the ratio of electric to total wave energy (Melrose 1980) defined by

$$R = \frac{1}{\omega \boldsymbol{e}^*_i \boldsymbol{e}_j \partial\Lambda^{\mathrm{H}}_{ij}/\partial\omega}, \tag{A18}$$

with $\boldsymbol{e} = \boldsymbol{\mathscr{E}}^{(0)}/|\boldsymbol{\mathscr{E}}^{(0)}|$. The velocity (A15b) can be interpreted as the group velocity in view of the following relation:

$$\frac{\partial\omega}{\partial\boldsymbol{k}} = -\frac{(\partial\Lambda^{\mathrm{H}}_{ij}/\partial\boldsymbol{k})\,\boldsymbol{e}^*_i\boldsymbol{e}_j}{(\partial\Lambda^{\mathrm{H}}_{lm}/\partial\omega)\,\boldsymbol{e}^*_l\boldsymbol{e}_m}. \tag{A19}$$

From equation (A14), growth or damping of the waves is determined by (A15c)–(A16), which can be derived by local approximation (Krall & Trivelpiece 1973, p. 425).